JOURNAL OF
Materials
CHEMISTRY

Intercalation and polymerisation of aniline within a tubular aluminosilicate

Vittorio Luca*†[a] and Stuart Thomson[b]

[a]Research School of Chemistry, The Australian National University, Canberra, ACT, 0200, Australia. E-mail: vlu@ansto.gov.au
[b]School of Chemistry, University of New South Wales, Sydney 2052, Australia

Received 27th January 2000, Accepted 26th May 2000
Published on the Web 18th July 2000

The intercalation and polymerization of aniline within the pores of a natural tubular Cu^{2+}-exchanged aluminosilicate clay known as halloysite is studied. The mesoscopic clay fibres have internal diameters of approximately 180 Å and lengths of up to 20 μm and can be deposited as films into which aniline is introduced from the vapour phase. The aniline composite was characterized by powder XRD, TGA, EPR, UV-Vis, XPS and IR spectroscopy. The present results confirm the presence of polyaniline on the internal and external surfaces of the halloysite tubes, thus indicating that the composite material could act as a molecular wire. The polyaniline initially sorbed onto the external surfaces is in a reduced state and evolves toward a more oxidized state as the duration of exposure of the film to aniline vapour increases.

Introduction

Chemists and materials scientists have long sought to alter the properties of molecular entities for use as molecular devices. Theoretical work[1] first proposed the use of individual molecules for rectification and unidirectional signal transmission. In the years following this study, there has been an increased focus on the synthesis of a large number of donor–acceptor molecules and their use as conducting nanostructures within porous substrates. This type of approach has the potential to produce novel materials in which the electronic and optical properties of the guest are modulated by the spatial and electronic properties of the host. The possibility of creating electronic devices of molecular dimensions such as wires, switches, sensors, and rectifiers has given scientists much to strive for. In this context, numerous attempts have been made to incorporate electro-active polymers within the intra-crystalline spaces of various hosts, and in doing so, give rise to novel hybrid electronic properties.

Of the known conducting polymers, polyaniline is unique as its conductivity can be switched on and off through control of chemical parameters such as the doping level. Unlike other conducting polymers where the conductivity increases to a saturation value, polyaniline undergoes several changes from conductor to insulator. There exist several forms that can be distinguished according to the proportions of oxidised and reduced units (x) as shown in Fig. 1. The following nomenclature has been given to the various oxidised forms: (1) leucoemeraldine ($x=0$), (2) protoemeraldine ($x=0.25$), (3) emeraldine base ($x=0.50$), (4) nigraniline ($x=0.75$), (5) pernigraniline ($x=1.0$). Polyaniline in the fully reduced form ($x=0$) is an insulator and then on mild oxidation becomes a conductor. Further oxidation results in the formation of the pernigranular form, an insulator.

To date, polyaniline has been intercalated into a variety of insulating host materials such as silicates,[2,3] uranium micas,[4] FeOCl,[5] hectorite,[6] zirconium phosphates,[7,8] double hydroxides,[9] layered semiconducting hosts such as V_2O_5[10] and MoS_2,[11] as well as network silicates such as zeolites,[12] and the recently discovered ordered mesoporous silicate MCM-41.[13] With the possible exception of MoS_2 and MCM-41,[14] these host materials are not available as large single crystals or tubules and therefore do not allow for macroscopic spatial alignment, although microscopic alignment within a crystallite has certainly been realised. This implies that their use as "molecular wires" may be limited.

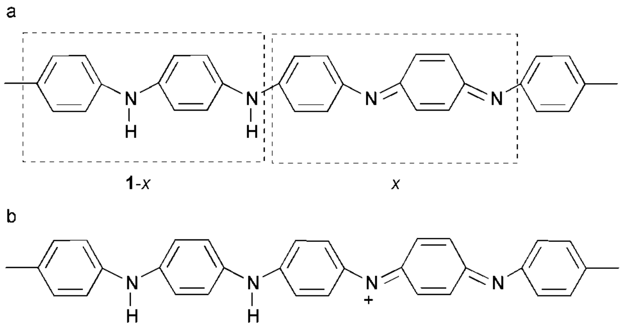

Fig. 1 Graphical representation of the polyaniline backbone (a) and the emeraldine salt depicted without a counter anion (b).

In this study, the intercalation and polymerization of aniline within a natural nanotubular aluminosilicate is addressed. The halloysite used is the same material recently described by Norrish.[15] Its structure is based on the dioctahedral (2/3 octahedral site occupancy) 1 : 1 layer structure of kaolinite and the structural formula determined by Norrish is $[Si_2Al_2Fe_{0.004}Mg_{0.004}Ca_{0.0016}K_{0.001}O_7]$. The layers curl into tubule structures with a spiral cross section resembling a roll of carpet, most likely due to the mismatch in the areas of the octahedral and tetrahedral sheet making up the 1 : 1 layer. In the hydrated state, this halloysite consists of uniform closely packed tubes exhibiting extremely large internal diameters of *ca.* 180 Å and relatively thin walls of 50–60 Å.[15] With a cation-exchange-capacity of about 20 meq 100 g^{-1}, and tubules exhibiting external diameter to length ratios of up to 1 : 1250, this halloysite would appear to be a promising host material for the formation of genuine molecular wires. Moreover, because of the mesoporosity, and to facilitate study of films in which the fibres are preferentially aligned in the plane of the film, we chose to introduce aniline from the vapour phase.

---

†Present address: Materials Division, Australian Nuclear Science and Technology Organisation, PMB 1, Menai 2234, Australia.

DOI: 10.1039/b000741m

Experimental

When the natural halloysite sample was dispersed in water to give a 1 wt.% suspension, a thixotropic gel formed. After this suspension was left standing for several weeks, films were formed from the top fraction of this gel in order to obtain purer material. A C, H, and N analysis of the purified material gave values of 0.24, 2.08, and 0.12 wt.% respectively indicating that a small amount of organic matter was present prior to exposure to aniline.

To polymerize polyaniline within halloysite, the halloysite first had to be exchanged with Cu(II) to allow the oxidative polymerisation of aniline to be driven by the Cu(II)/Cu(I) redox couple. This was done by stirring the purified 1% suspension with a 0.5 M Cu(II) solution for 24 h followed by dialysis to remove excess Cu(II). A Cu(II)-exchanged film in which the fibres were preferentially oriented parallel to the film surface was formed by allowing the suspension to dry in ambient air on a plastic or Al sheet from which the halloysite film was later separated. The films were then exposed to aniline vapour for various times by placing them in an open glass vial (5 mL) contained within a larger sealed vessel at the bottom of which were several millilitres of aniline. The aniline was freshly distilled over granulated zinc. The Cu(II) contained within the halloysite promotes the oxidative polymerization of the aniline monomers. This is visually apparent from the change in the colour of the Cu(II)–halloysite films from grey to red. A C, H, and N analysis of the sample after prolonged exposure gave values of 4.43, 2.36 and 0.57% respectively. Similar transition metal ion promoted oxidation reactions have been used in the polymerisation of aniline monomers in other Cu^{2+}-exchanged silicate hosts,[16] Cu^{2+}-exchanged layered phosphates,[17] V_2O_5 where the V(V)/V(IV) redox system was exploited[18] and in FeOCl where the Fe(III)/Fe(II) system provided the driving force.[19]

Transmission electron microscope (TEM) images were obtained at 300 kV on a Philips EM430 instrument with samples supported on holey carbon grids.

X-Ray diffraction patterns were recorded on a Siemens D5000 diffractometer using Cu-K_α radiation.

Conductivities of the halloysite and PANI–halloysite films were measured by a conventional four-point-probe technique.

X-Ray photoelectron spectroscopy (XPS) measurements were performed on a Kratos XSAM 900 instrument incorporating a non-monochromated Mg source. Initial spectra were collected from the surface of the as-loaded sample, which was then subjected to argon ion etching, and subsequent analyses performed. Copper halloysite samples were referenced to adventitious carbon (C1s = 284.8 eV), while subsequent measurements upon intercalated samples were referenced to the oxygen peak (O1s = 532.1 eV).

Electron paramagnetic resonance (EPR) spectra were collected on a Varian V-4502 spectrometer interfaced to a PC data acquisition system and equipped with an Oxford Instruments flow cryostat. FTIR spectra of PANI–halloysite films were acquired in transmission mode on a Perkin-Elmer PE1800 spectrometer. UV-Vis spectra were recorded on a Varian Cary 500 spectrometer without any sample in the reference beam. Thermogravimetric analyses were recorded using a Stanton Redcroft TG-750 thermobalance in a flow of air using a heating rate of 10 °C min^{-1}.

Results and discussion

Exposure of the Cu(II)-exchanged halloysite film (light blue in colour) to aniline vapour resulted in distinct colour changes. During the initial hours of exposure the sample turned grey, and upon further exposure the formation of a deep burgundy color was observed. The UV-Vis spectrum of Cu(II)–halloysite, after 48 h of exposure to aniline vapour, showed a single broad absorption at 500 nm (2.6 eV) and a weak shoulder at about 340 nm (3.8 eV) (Fig. 2). A similar optical spectrum has been observed for polyaniline films deposited from the vapour phase onto silica substrates.[20] In that system the optical spectrum was attributed to polyaniline units with chain lengths shorter than in 'conventional' polyaniline but longer than five-ring oligomers. The spectrum of PANI–halloysite is also very similar to that of the insulating form of polyaniline intercalated within layers of a mica-type silicate (fluorohectorite) through the vapour phase.[16] In this polyaniline–fluorohectorite composite the polyaniline was initially deposited in the insulating state, exposure to HCl vapour being necessary for reduction and hence increased conductivity. The 500 nm absorption of polyaniline–fluorohectorite was attributed to charge transfer from the benzoid to the quinoid segments, while the shoulder at 340 nm is indicative of $\pi \rightarrow \pi^*$ transitions in reduced units of polyaniline.[21] Because of the small particle size of this silicate, polyaniline units must necessarily be very short. The optical spectrum of PANI–halloysite is therefore indicative of short polyaniline chains with x between 0.5 and 1. Such short chains are apparently due to a limitation on chain growth afforded by the vapour deposition method while the high value of x is due to a relatively oxidizing environment and low surface acidity.

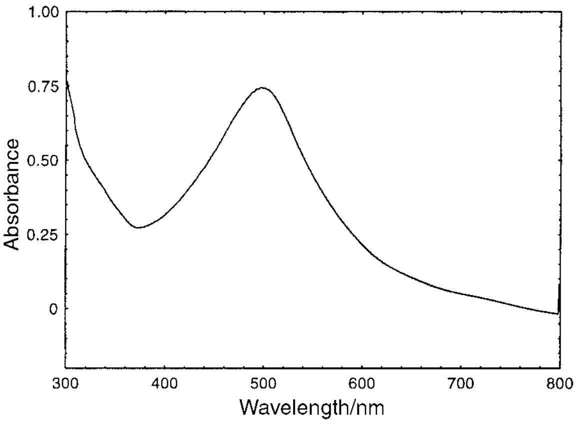

Fig. 2 UV-Vis spectrum of PANI–halloysite films exposed to aniline vapour for 48 h.

In an effort to ascertain the location of polyaniline within the halloysite, aniline intercalation was monitored by powder XRD. Fig. 3a shows that prior to exposure, the film gave a basal reflection at 8.0 Å. This has been attributed to combined diffraction from the interlayer region (~7.2 Å), the separation between the inner collapsed tube walls (~5 Å), and the separation between adjacent particles (~5 Å).[15] On exposure to aniline, the relative intensity of the shoulder assigned to the 7.1 Å interlayer repeat was observed to increase slightly (Fig. 3b,c). The removal of residual adsorbed water from the tube interiors and the intercalation of aniline may be responsible for this effect. For comparison, the XRD pattern of an oriented film of the Cu(II)-doped layered montmorillonite clay that was similarly treated with aniline is shown in Fig. 3d. This material gave a basal X-ray diffraction peak at 15.2 Å which represents an expansion of the inter-layer space by approximately 5.4 Å, which is consistent with the dimensions of one mono-layer of polyaniline lying flat within the inter-layer space. If aniline were entering the halloysite inter-layers, a similar layer expansion would have been observed. This was not the case, indicating that the intercalation of aniline can only occur on the external or internal tube surfaces.

The FTIR spectra of a Cu(II)-exchanged halloysite film before and after exposure to aniline for 10 hours are shown in Fig. 4. The unexposed film contains well resolved bands at 3700 and 3629 cm^{-1} due to two different populations of OH groups superimposed on a broad absorption due to adsorbed water. Sorption of aniline over a 10 h period does not result in any

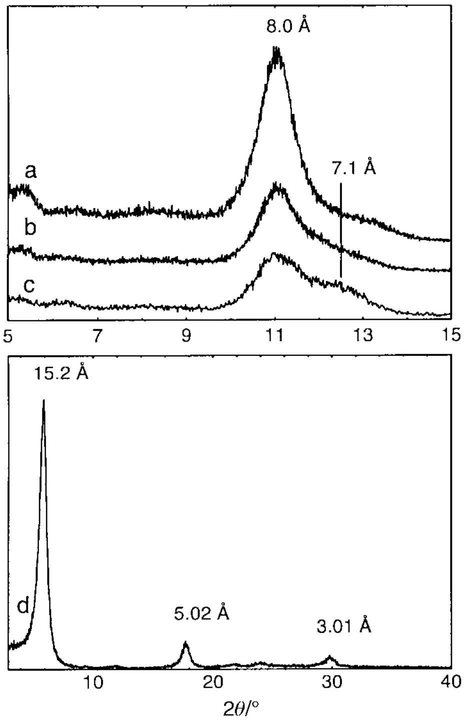

Fig. 3 XRD patterns of (a) Cu(II)–halloysite film, (b) Cu(II)–halloysite film exposed to aniline vapour for 24 h, (c) Cu(II)–halloysite film exposed to aniline vapour for 2 weeks and (d) Cu(II)–montmorillonite clay film after exposure to aniline vapour for several weeks.

significant change to the spectrum in this region. The unexposed sample also shows some weak features in the 1700–1500 cm^{-1} range where the bending vibrations of adsorbed water are expected.

Intercalation of aniline results in the formation of peaks between 1700–1200 cm^{-1} that are characteristic of polyaniline (Table 1). All forms of polyaniline have intense infrared bands near 1500 cm^{-1} (attributed to the 8a mode (Wilson's notation) from the phenyl C–C breathing mode) and 1300 cm^{-1} (attributed to the 14 mode from the phenyl–N stretch). However, while pernigraniline and the emeraldine base also have an intense band at 1600 cm^{-1}, leucoemeraldine does not. These intense vibrational modes near 1600 cm^{-1} have been attributed to the quinoid ring structure (8a mode of the quinoid ring).[22] Thus the ratio I_{1600}/I_{1500} gives an estimate of the degree of oxidation (the value of x).

The presence of weak peaks at 3386 and 3319 cm^{-1} can be assigned to the $\nu_{\text{sym}}(\text{NH}_2)$ modes of aniline. The existence of these peaks at values shifted from those of neutral aniline, which typically exhibit values of 3481 and 3360 cm^{-1},[7] suggests that aniline is co-ordinated to metal centres or bound to the halloysite surface by H-bonding. Analysis of the OH stretching region (the result of O–H groups associated with octahedral and tetrahedral sheets of the 1 : 1 layers) for aniline–hydroxyl interactions proved difficult because the number of hydroxyl groups associated with the internal surfaces of the tubes is small in comparison to the number of hydroxyl groups associated with the inter-layer regions, which we have shown are inaccessible to aniline. Therefore, it was deemed unlikely that such interactions would be observed, and this was indeed the case.

Fig. 5 shows the effect of extended aniline exposure on the FTIR spectra of the Cu(II)–halloysite film. A mixture of polymer units was present throughout 120 hours of exposure, although several important changes were observed. The most obvious change was the increase in intensity of the 1468 cm^{-1} band relative to the 1499 cm^{-1} band and the associated lower frequency shoulder at 1490 cm^{-1} with increasing contact time. This red-shifting of ring vibrations is diagnostic of the transition from leucoemeraldine ($x = 0$) and emeraldine base forms ($x = 0.5$) toward the pernigraniline form ($x = 1$),[23] and therefore indicates an increase in the ratio of oxidized to reduced polyaniline units within the sample. It is noteworthy that the shoulder at 1582 cm^{-1}, barely visible during the early stages of reaction, and diagnostic of quinone diimine radical cations,[24,25] also increased in intensity with contact time.

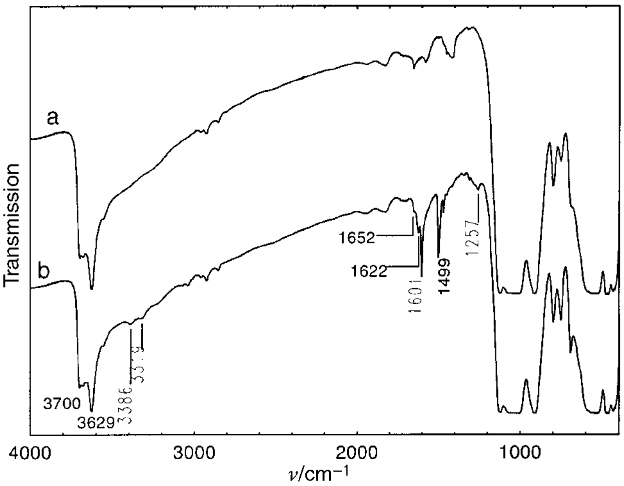

Fig. 4 FTIR spectra in the range 4000–400 cm^{-1} before (a) and after (b) exposure to aniline vapour for 10 h.

The IR spectrum of the halloysite sample equilibrated with aniline for two weeks was similar to that of polyaniline intercalated within mordenite.[26] In mordenite, bands were observed at 1581, 1497, 1310, and 1246(sh) cm^{-1} and in contrast the colour of the sample was blue. The IR bands in halloysite appeared at 1582, 1472, 1300 cm^{-1}, and a weak shoulder was present at 1258 cm^{-1}, with the sample exhibiting a deep red colour. The variation in IR peak positions, together with the distinct optical spectrum, suggests that the interaction of polyaniline within the host differs from that of mordenite.

As discussed above, to obtain an estimate of the value of x from the FTIR data of Fig. 5, the I_{1600}/I_{1500} ratio could be used. To determine I_{1600}/I_{1500}, the spectra were converted to absorbance by taking the spectrum of the unexposed sample as the background. These spectra were then decomposed into individual components and I_{1600}/I_{1500} was determined. For the spectrum of the sample exposed for 10 h a value of 0.2 was obtained while the spectrum of the sample exposed for 120 h gave a value of 1.5. It is therefore apparent that the polyaniline is initially in a reduced state, but within 120 h, significant conversion to the oxidized form occurs.

The TEM images of halloysite samples before and after exposure to aniline vapour are shown in Fig. 6a and b. Initial images showed that the tubes of PANI–halloysite were not as transparent to electrons as the untreated material. Although PANI–halloysite appeared more ribbon-like than the untreated material, a defined wall structure was discernible. Furthermore, the electron diffraction pattern of the untreated sample was reasonably intense showing a definite 7 Å repeat distance, but it was not possible to obtain a diffraction pattern from the aniline treated material. These observations are consistent with the location of the polymer either within the tubular voids of halloysite or possibly on the surfaces of the ribbons.

Supporting the hypothesis that polyaniline resides within the halloysite tubes is the fact that evacuation and subsequent dehydration of halloysite prior to aniline exposure resulted in a dramatic increase in the time required for the red coloration of the sample to become apparent. This suggests that in the air-dried sample the tubes are more open due to the presence of residual water and this facilitates the diffusion of aniline and its subsequent polymerisation.

Table 1 Major absorption bands for bulk polyanilines and polyaniline intercalates[a]

Compound	Ring stretching modes[b]								Reference
L				1280			1501s	1612w	37
EB				1288			1501s	1593s	37
			1247		1302		1501s	1568s	38
ES			1246		1300		1493s	1578s	37
							1486s	1568s	38
P					1315m		1480s	1570s	22
PANI–Y		1246			1315		1497s	1583s	26
PANI–hal (120 h)	1206	1256		1294		1330	1469	1583	This work
						1370	1490	1601	
							1498	1624	
PANI–hal (>2 weeks)	1206	1256		1296		1332	1473	1582	This work
							1420	1603	

[a] L = Leucoemeraldine form, EB = emeraldine base form, ES = emeraldine salt form, P = pernigraniline, PANI–Y = polyaniline intercalated zeolite-Y, PANI–hal = polyaniline intercalated halloysite. [b] Red shift of the ring stretching mode at 1500 cm^{-1} to *ca.* 1490 cm^{-1} is a signature for the conversion of quinoid rings to benzenoid rings.

From XPS measurements performed on Cu(II)-exchanged halloysite, the following binding energies were obtained after referencing to the C1s = 284.8 eV of adventitious carbon; Al2p = 74.7 eV, Si2p = 103.1 eV, and O1s = 532.1 eV. Subsequent referencing of the aniline intercalated spectra was performed using the O1s peak (532.1 eV). This procedure has been used previously[27] for microporous materials and was deemed a more satisfactory method for charge correction because of the difficulty in separating adventitious carbon from the C1s peaks of aniline.

The N1s spectrum obtained from the outer surface of the Cu(II)-doped halloysite exposed to aniline vapour for two weeks is shown in Fig. 7. A minimum of three peaks were required to achieve a satisfactory fit to the experimental envelope. These peaks were found to have binding energies of 398.8 eV, 400.2 eV, and 402.1 eV. The former two peaks can be assigned to –N=Q and –HN–ϕ respectively (where Q = quinone and ϕ = benzene) with the latter peak most likely due to a combination of the emeraldine salt and ionic radicals (–HN$^+$–ϕ). These assignments are based on those described in previous studies of bulk polyaniline[28–31] and film samples.[32] The existence of the peak at 402.1 eV may indicate an interaction of polyaniline with the host, although similar XPS spectra have been observed in bulk polyaniline samples.[28] The ratio of the area of the peak assigned to –HN–ϕ to that assigned to –N=Q gives a further estimate of the value of *x* in Fig. 1. From the peak decomposition, this ratio is close to one, indicating that the polyaniline on the outer surfaces is in an oxidized state, which is consistent with the FTIR and optical data. Efforts to probe the chemical nature of polyaniline and Cu within the tubules by Ar ion etching was not possible because etching of the surface by argon ions results in chemical changes to the polymer and the Cu.

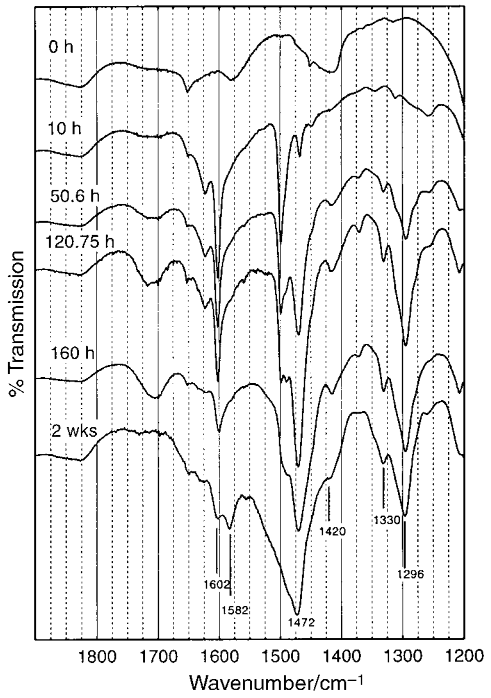

Fig. 5 FTIR spectra of film after increasing exposure to aniline vapour.

XPS measurements performed on the aniline intercalated materials showed a carbon : nitrogen ratio of 6 : 1. The carbon content remained constant after Ar ion etching suggesting a uniform composition throughout the profile of the stack of

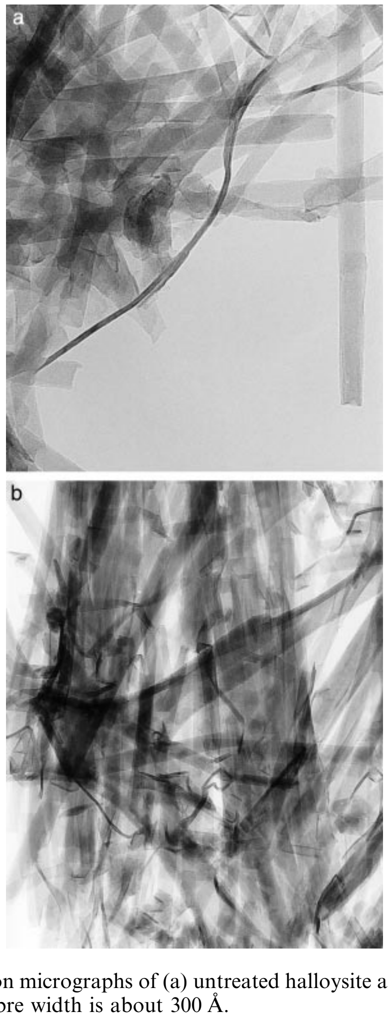

Fig. 6 Electron micrographs of (a) untreated halloysite and (b) PANI–halloysite. Fibre width is about 300 Å.

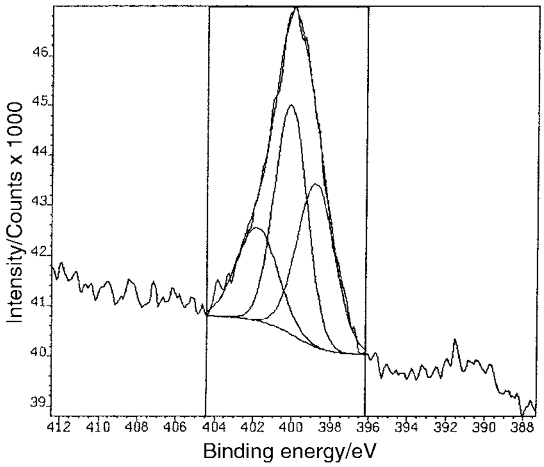

Fig. 7 N1s XPS spectrum of PANI–halloysite after exposure to aniline vapour for 2 weeks.

oriented fibres.

Thermogravimetric analysis (TGA) of the non-intercalated sample equilibrated at a relative humidity of 30% resulted in a sharp weight loss at 100 °C accounting for about 7% of the total sample weight. In contrast, the TGA of the sample equilibrated in aniline vapour for two weeks showed no low temperature weight loss and instead lost 5.5% of its total weight gradually over a temperature range of several hundred degrees. From these data, the amount of sorbed aniline corresponds to an aniline : $Al_2Si_2O_5(OH)_4$ ratio of 0.15 : 1. That the sorption of aniline results in removal of residual inter-layer water is confirmed by the FTIR spectrum which showed a slight reduction in the intensity in the O–H stretching and bending vibrations of adsorbed water with increased exposure to aniline vapour.

Analyses of C, H, and N were obtained of both the untreated and PANI–halloysite. In the untreated halloysite, C = 0.24, H = 2.08, and N = 0.12 wt.%. The small content of C and N is most likely due to organic impurities present within the natural sample. This is confirmed by the presence of small traces of organic impurities in the IR spectrum of the untreated halloysite sample shown in Fig. 4. The analysis of the PANI–halloysite gave C = 4.43, H = 2.36 and N = 0.57 wt.%. This compares well with the weight loss observed in the TGA analysis. A direct comparison of the C : N ratio in the PANI–halloysite sample yielded a figure of 7.7 : 1, and subtracting out the residual C and N levels contained in the untreated halloysite yielded a C : N ratio of 9 : 1. This is somewhat higher than the C : N ratio obtained by XPS which was close to the calculated value for polyaniline.

Cu(II)-doped films that had been equilibrated at 30% RH gave the EPR spectra shown in Fig. 8a and b. A signal due to an Fe(III) impurity can be observed at $g = 4.2$ while the Cu(II) ion gives g-tensor parameters of $g_{\|} = 2.36$, $A_{\|} = 146$ G, and $g_{\perp} = 2.05$. The Cu(II) spectrum is typical of the hydrated Cu(II) ion in an axial environment. The Cu(II) spectrum showed a pronounced dependence on the orientation of the Cu(II)-exchanged halloysite film with respect to the external magnetic field. When the film was perpendicular to the external field, the parallel g-tensor components are emphasized, and in the parallel film orientation, the perpendicular components are emphasized. Similar results have been described for preferentially oriented Cu(II)-exchanged smectite clay films.[33] Like the Cu(II) spectrum the resonance assigned to Fe(III) also showed significant orientation dependence. From the orientation dependence of the Cu(II) resonance the principal g-tensor axis of the Cu(II)–aquo complexes is perpendicular to the long axis of the tubes. Also apparent in these spectra are three lines of a six-line spectrum of an Mn(II) impurity. The orientation dependence observed for the Cu(II) and Fe(III) spectrum for the air-dried Cu(II)–halloysite film suggests that prior to exposure to aniline the aspect ratio of the tubes is greater than one since perfect tubes, with an aspect ratio of one, would not be expected to produce such orientation dependence. That is, the tubes are at least partially collapsed on air-drying and prior to exposure to aniline.

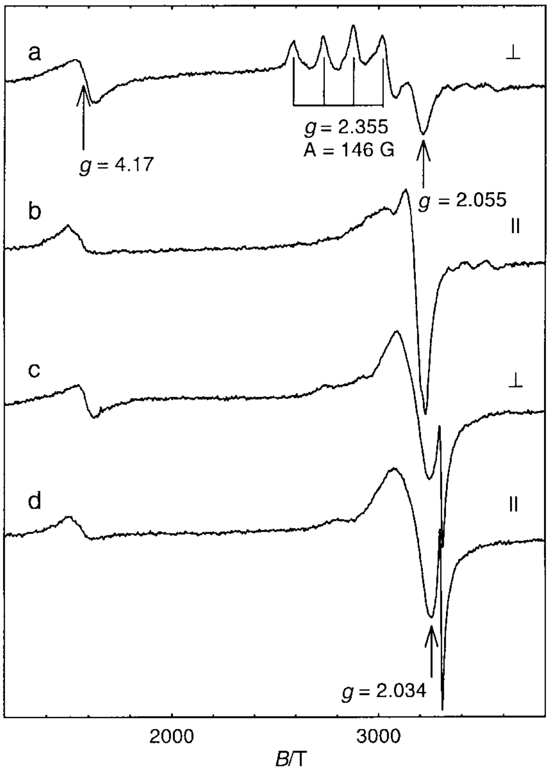

Fig. 8 EPR spectra of Cu(II)-exchanged halloysite film perpendicular (a) and parallel (b) to the external magnetic field and PANI–halloysite film oriented perpendicular (c) and parallel (d) to the external field.

Exposure of the Cu(II)-doped halloysite film to aniline vapour for two weeks produced the spectra shown in Fig. 8c and d when the films are aligned respectively perpendicular and parallel to the magnetic field. The resonances at $g = 2.034$ are those of the Cu(II) originally exchanged onto the surfaces and resemble, in both the weak orientation dependence and structure, the spectrum of vacuum dehydrated samples. This suggests that the intercalation of polyaniline results in dehydration which causes a dramatic change in the Cu(II) environment presumably due to co-ordination to the surfaces. The much reduced orientation dependence of both the Cu(II) and Fe(III) signals indicates that the aspect ratio is closer to one than it was prior to the introduction of aniline. These results provide evidence that at least partial intercalation of aniline has been achieved.

The structureless resonance at $g = 1.996$ with an estimated linewidth of around 20–50 G is not from Cu(II), but is probably from radicals associated with polyaniline which usually give a resonance close to $g = 2.000$. This resonance is not observed in samples equilibrated for less than 48 h. Polyaniline in the conducting (doped) state gives rise to an EPR signal from radical cations. These signals have a narrow linewidth and exhibit hyperfine splitting due to coupling of the unpaired electron spin to other atoms in the polyaniline molecule.[34,35] No such splittings were observed in the present case, suggesting delocalization of the electron along the length of the polyaniline chain. The presence of such radical species is confirmed by the appearance of a band at 1583 cm^{-1} in the FTIR spectrum of the sample equilibrated in aniline for two weeks.

Evidence for refuting the possibility that complexes are forming between aniline ligands and Cu(II) is also provided by the EPR spectra. The interaction of strong bases, such as ammonia and pyridine, with Cu(II) in smectite clays gives rise to well resolved superhyperfine splitting of the Cu(II) EPR spectrum.[36] Such splittings were not observed here indicating that aniline polymerisation was favoured over complex formation. This interpretation is also supported by the absence of IR bands due to unbound neutral aniline in the intercalated halloysite sample. Efforts were made to observe weak hyperfine interactions between Cu(II) and aniline nitrogen atoms not directly coordinated to the metal centre using the electron spin echo envelope modulation technique and none were detected.

The resistivity values of Cu(II)–halloysite and PANI–halloysite that was cut from the same piece of film were 5×10^8 and 3×10^{10} Ω cm^{-2} respectively. The high resistivity of the PANI–halloysite film is consistent with previous observations that polyaniline coating the exterior of the tubes is in an oxidized, and therefore insulating, state. Lower resistivity of the Cu(II)–halloysite compared to the PANI–halloysite can also be a reflection of the higher water content of the former sample and the fact that mobile exchangeable Cu(II) cations are able to facilitate a small degree of charge transport.

Conclusions

The vapour phase sorption and polymerization of aniline on the internal and external surfaces of Cu(II)-exchanged halloysite has been monitored using a variety of techniques. Evidence has been put forward suggesting that at least some of the polymers are present within the tubular structure of Cu(II)-exchanged halloysite. Techniques such as IR and UV-Vis spectroscopy have shown the polyaniline formed on the surfaces of halloysite displays similar characteristics to bulk polyaniline. A conversion from the predominantly reduced to the predominantly oxidized form is observed as a function of exposure time.

The ability of halloysite to be easily prepared as films, and the ability to grow polyaniline within its tubular structure, is an encouraging development in the search for suitable molecular devices. However, halloysite is but one of a large number of silicate minerals that adopt tubular structures including the serpentine group of minerals of which the magnesium silicate crysotile (asbestos) is a member. Nickel and cobalt silicate analogues of crysotile have been synthesised and such materials may react quite differently with aniline and the monomers of other intrinsically conducting polymers to give composite materials with novel properties. Further studies should address the possibility of the intercalation and subsequent polymerization of aniline by other means including from the liquid phase from a variety of solvents.

Acknowledgements

The authors are most grateful to Dr Keith Norrish of the Division of Soils, CSIRO, Glen Osmond, South Australia for supplying the sample. We are also grateful to Dr Chennupati Jagadish of the Electronic Materials and Engineering Department of the Research School of Physical Sciences and Engineering at The Australian National University for the four-point-probe measurements and Dr John FitzGerald of the Research School of Earth Sciences at The Australian National University for the electron microscope images.

References

1 A. Aviran and M. A. Ratner, *Chem. Phys. Lett.*, 1974, **29**, 277.
2 P. Cloos, C. Moreale, C. Braers and C. Badot, *Clay Miner.*, 1979, **14**, 307.
3 C. Moreale, P. Cloos and C. Badot, *Clay Miner.*, 1985, **20**, 29.
4 M. Martinez-Lara, J. A. Marea-Aranda, L.-M. Real and S. Bruque, *J. Incl. Phenom. Mol. Recognit. Chem.*, 1990, **9**, 287.
5 M. G. Kanatzidis, C.-G. Wu, H. O. Marcy, D. C. DeGroot and C. R. Kannewurf, *Adv. Mater.*, 1990, **2**, 364.
6 T. L. Porter, D. Thompson, M. Bradley, M. P. Eastmann, M. E. Hagerman, J. L. Attuso, A. E. Votava and E. D. Bain, *J. Vac. Sci. Technol. A*, 1997, **15**, 500.
7 D. J. Jones, R. E. Meijad and J. Roziere, *Supramolecular Architecture*, ed. T. Bein, American Chemical Society, Washington DC, 1992, p. 220.
8 M.-H. Herzog-Cance, D. J. Jones, R. El Mejjad, J. Roziere and J. Tomkinson, *J. Chem. Soc., Faraday Trans.*, 1992, **88**, 2275.
9 T. Challier and R. C. Slade, *J. Mater. Chem.*, 1994, **4**, 367.
10 Y.-J. Liu, D. C. DeGroot, J. L. Schindler, C. R. Kannewurf and M. G. Kanatzidis, *Chem. Mater.*, 1991, **3**, 992.
11 M. G. Kanatzidis, R. Bissessur, D. C. DeGroot, J. L. Schindler and C. R. Kannewurf, *Chem. Mater.*, 1993, **5**, 595.
12 P. Enzel and T. Bein, *Chem. Mater.*, 1992, **4**, 819.
13 C.-G. Wu and T. Bein, *Science*, 1994, **264**, 1757.
14 F. Marlow, M. D. McGehee, D. Zhao, B. F. Chmelka and G. D Stucky, *Adv. Mater.*, 1999, **11**, 632.
15 K. Norrish, *Proceedings of the 10th International Clay Conference, Adelaide, Australia, July 18–23, 1993*, ed. G. J. Churchman, R. W. Fitzpatrick and R. A. Eggleton, CSIRO Publishing, Melbourne, Australia, 1995, p. 275.
16 V. Mehrotra and E. P. Giannelis, *Solid State Commun.*, 1991, **77**, 155.
17 P. Maireles-Torres, P. Olivera-Pastor, E. R. Castellon and A. J. Lopez, *J. Incl. Phenom. Mol. Recognit. Chem.*, 1992, **14**, 327.
18 M. G. Kanatzidis, C.-G. Wu, H. O. Marcy and C. R. Kannewurf, *J. Am. Chem. Soc.*, 1989, **111**, 4139.
19 M. G. Kanatzidis, C.-G. Wu, H. O. Marcy, D. C. DeGroot and C. R. Kannewurf, *Adv. Mater.*, 1990, **2**, 364.
20 K. Uvdal, M. Lögdlund, P. Dannetun, L. Bertilsson, S. Stafström, W. R Salaneck, A. G. MacDiarmid, A. Ray, E. M. Scherr, T. Hjertberg and A. J. Epstein, *Synth. Met.*, 1989, **29**, E451.
21 A. J. Epstein, J. M. Ginder, F. Zuo, H. S. Woo, D. B. Tanner, A. F. Richter, M. Angelopoulos, W. S. Huang and A. G. MacDiarmid, *Synth. Met.*, 1987, **13**, 63.
22 S. Quillard, G. Louarn, S. Lefrant and A. G. MacDiarmid, *Phys. Rev. B: Condens. Matter*, 1994, **50**, 12498.
23 Y. Furkukawa, T. Hara, Y. Hyodo and I. Harada, *Synth. Met.*, 1986, **16**, 189.
24 L. W. Shaklette, J. F. Wolf, S. Gould and R. H. Baughman, *J. Chem. Phys.*, 1988, **88**, 3955.
25 A. P. Monkman, D. Bloor, G. C. Stevens, J. C. H. Stevens and P. Wilson, *Synth. Met.*, 1989, **29**, E277.
26 P. Enzel and T. Bein, *J. Phys. Chem.*, 1989, **93**, 6270.
27 R. B. Borade and A. Clearfield, *Appl. Catal. A: Gen.*, 1992, **80**, 59.
28 A. P. Monkman, G. C. Stevens and D. Bloor, *J. Phys. D: Appl. Phys.*, 1991, **24**, 736.
29 X.-R. Zeng and T.-M. Ko, *J. Polym. Sci.: Part B: Polym. Phys.*, 1997, **35**, 1993.
30 K. L. Tan, B. T. G. Tan, E. T. Kang and K. G. Neoh, *J. Chem. Phys.*, 1991, **94**, 5382.
31 K. L. Tan, E. T. Kang and K. L. Tan, *J. Phys. Chem.*, 1997, **101**, 726.
32 N. G. Neoh, E. T. Kang and K. L. Tan, *J. Phys. Chem.*, 1997, **101**, 726.
33 D. M. Clementz, T. J. Pinnavaia and M. M. Mortland, *J. Phys. Chem.*, 1973, **77**, 196.
34 S. H. Glarum and J. H. Marshall, *J. Electrochem. Soc.*, 1987, **134**, 2160.
35 S. H. Glarum and J. H. Marshall, *J. Phys. Chem.*, 1988, **92**, 2160.
36 V. Luca and L. Kevan, *J. Phys. Chem.*, 1992, **96**, 3391.
37 Y. H. Kim, C. Foster, J. Chiang and A. J. Heeger, *Synth. Met.*, 1988, **26**, 49.
38 R. P. McCall, M. G. Roe, J. M. Ginder, T. Kusumoto, A. J. Epstein, G. E. Asturias, E. M. Sheerr and A. G. MacDiarmid, *Synth. Met.*, 1989, **29**, E433.